AD-A104 518 AIR FORCE GEOPHYSICS LAB HANSCOM AFB MA F/G 4/1
HIGH LATITUDE ELECTRON DETECTORS ON SATELLITE P78-1: PRELIMINAR--ETC(U)
MAY 81 R P VANCOUR
UNCLASSIFIED AFGL-TR-81-0131 NL

LEVEL II

AFGL-TR-81-0131
ENVIRONMENTAL RESEARCH PAPERS, NO. 744

AD A104518

High Latitude Electron Detectors on Satellite P78-1: Preliminary Data Results

ROGER P. VANCOUR

4 May 1981

Approved for public release; distribution unlimited.

DTIC
ELECTE
SEP 24 1981
S
D
D

SPACE PHYSICS DIVISION PROJECT 7601
AIR FORCE GEOPHYSICS LABORATORY
HANSCOM AFB, MASSACHUSETTS 01731

AIR FORCE SYSTEMS COMMAND, USAF

DTIC FILE COPY

This report has been reviewed by the ESD Information Office (OI) and is releasable to the National Technical Information Service (NTIS).

This technical report has been reviewed and is approved for publication.

FOR THE COMMANDER

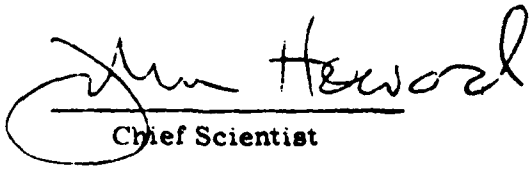

Chief Scientist

Qualified requestors may obtain additional copies from the Defense Technical Information Center. All others should apply to the National Technical Information Service.

Unclassified

SECURITY CLASSIFICATION OF THIS PAGE (When Data Entered)

REPORT DOCUMENTATION PAGE

READ INSTRUCTIONS BEFORE COMPLETING FORM

1 REPORT NUMBER: AFGL-TR-81-0131	2 GOVT ACCESSION NO: AD-A104 578
3 RECIPIENT'S CATALOG NUMBER	
4 TITLE (and Subtitle): HIGH LATITUDE ELECTRON DETECTORS ON SATELLITE P78-1: PRELIMINARY DATA RESULTS.	5 TYPE OF REPORT & PERIOD COVERED: Scientific Final Rept.
	6 PERFORMING ORG. REPORT NUMBER: ERP No. 744
7 AUTHOR(s): Roger P. Vancour	8 CONTRACT OR GRANT NUMBER(s)
9 PERFORMING ORGANIZATION NAME AND ADDRESS: Air Force Geophysics Laboratory (PHG) Hanscom AFB Massachusetts 01731	10 PROGRAM ELEMENT, PROJECT, TASK AREA & WORK UNIT NUMBERS: 62101F 7601 0903 17 09
11 CONTROLLING OFFICE NAME AND ADDRESS: Air Force Geophysics Laboratory (PHG) Hanscom AFB Massachusetts 01731	12 REPORT DATE: 4 May 1981
	13 NUMBER OF PAGES: 29
14 MONITORING AGENCY NAME & ADDRESS (if different from Controlling Office): AFGL-TR-81-0131, AFGL-ERP-744	15 SECURITY CLASS. (of this report): Unclassified
	15a DECLASSIFICATION/DOWNGRADING SCHEDULE

16 DISTRIBUTION STATEMENT (of this Report)

Approved for public release; distribution unlimited.

17 DISTRIBUTION STATEMENT (of the abstract entered in Block 20, if different from Report)

18 SUPPLEMENTARY NOTES

19 KEY WORDS (Continue on reverse side if necessary and identify by block number)

P78-1 satellite
Electron electrostatic analyzers
Aurora
Precipitating electrons

20 ABSTRACT (Continue on reverse side if necessary and identify by block number)

Air Force satellite P78-1 carries several experiments investigating solar activity and charged particle and electromagnetic radiation measurements. One of these experiments consists of a set of electrostatic analyzers to collect electrons from 50 eV to 20 KeV in 16 channels. The sensors are exactly the same as the SSJ/3 sensor on DMSP satellites.

Since the satellite is spinning at a rate of 11 ± 1 rpm, complete pitch angle information is obtained in ≈ 5.45 sec by each of the two sensors which

DD FORM 1 JAN 73 1473

Unclassified

SECURITY CLASSIFICATION OF THIS PAGE (When Data Entered)

409578

20. Abstract (Continued)

are 90^{0} apart. Three passes are reported, showing where each pass is during a different intensity of magnetic activity.

Oval boundaries, spectral shapes, and total energy fluxes are determined and compared to the results of others. Results from the two sensors are compared to each other.

Accession For
NTIS GRA&I
DTIC TAB
Unannounced
Justification
By
Distribution/
Availability Codes
Dist | Avail and/or Special
A

Contents

1. INTRODUCTION 7

2. DESCRIPTION OF ELECTROSTATIC ANALYZERS 8

3. RESULTS OF MEASUREMENTS FROM THREE PASSES 11

3.1 Quiet Time (Rev 270, Kp = 0_+), 14 March 1979 11
3.2 Moderate Activity (Rev 220, Kp = 3_+), 11 March 1979 17
3.3 Intense Activity (Rev 499, Kp = 7_-), 29 March 1979 21

4. CONCLUDING REMARKS 28

Illustrations

1. P78-1 Satellite 8

2. Trajectory in Northern Auroral Zone for Rev 270, 14 March 1979 12

3. Electron Data from Rev 270, 14 March 1979, During a Magnetic Quiet Time, Kp = 0_+ 13

4a. Differential Electron Spectra From Both Detectors at Corrected Geomagnetic Latitude 70.7°, Northern Nightside Auroral Oval, Rev 270, 14 March 1979. 15

4b. Same as 4a Except Electrons are not Field-Aligned but Were Collected Simultaneously With Approximately Equal Pitch Angles for Both Detectors 15

DTIC
SEP 1031
D

Illustrations

5a. Differential Electron Spectrum Taken at Corrected Geomagnetic Latitude 69.0°, Rev 270 16

5b. Differential Electron Spectrum From Detector 2 Taken at Corrected Geomagnetic Latitude 68.5°, Rev 270 16

6. Trajectory in Northern Auroral Zone for Rev 220, 11 March 1979 18

7. Electron Data from Rev 220, 11 March 1979, During a Magnetically Moderate Time, Kp = 3_+ 19

8a. Differential Electron Spectra From Both Detectors Taken at Corrected Geomagnetic Latitude 66.4°, Northern Nightside Auroral Oval, Rev 220 20

8b. Same as 8a Except Electrons Are Not Field-aligned but Were Collected Simultaneously With Approximately Equal Pitch Angles for Both Detectors 20

9. Trajectory in Southern Auroral Zone for Rev 499, 29 March 1979 22

10. *Electron Data From Rev* 499, 29 March 1979, During a Magnetic Storm Time, Kp = 7_- 23

11. Differential Electron Spectra From Both Detectors at Corrected Geomagnetic Latitude 56.0° South, Near Equatorward Edge of Nightside Oval, Rev 499 24

12. Differential Electron Spectrum From Detector 1 Taken at Corrected Geomagnetic Latitude 59.3°, Rev 499 24

13. Differential Electron Spectra From Detector 2 Taken During Three Successive Rotations of the Satellite 25

14. Plot of Electron Energy Values Where Maximum Flux Occurred Versus Universal Time in Seconds, Rev 499, Southern Nightside Auroral Oval, Active Region 26

15. Differential Electron Spectrum From Detector 1 Taken at Corrected Geomagnetic Latitude 62.6°, Rev 499 26

16. Differential Electron Spectra From Both Detectors Taken at Corrected Geomagnetic Latitude 64.8°, Southern Nightside Auroral Oval, Rev 499 27

17. Differential Electron Spectrum From Detector 1 Taken at Corrected Geomagnetic Latitude 65.6°, Rev 499 28

Tables

1. The Conversion Factor, Mid-Energy, and Energy Width for Each Energy Channel

2. Rev 270 (Kp = 0_+). CGM Latitudes for Dayside and Nightside Auroral Oval Boundaries 14

3. Rev 220 (Kp = 3_+). CGM Latitudes for Equatorward Auroral Oval Boundaries 17

4. Rev 499 (Kp = 7_-). CGM Latitudes for Dayside and Nightside Auroral Oval Boundaries

High Latitude Electron Detectors on Satellite P78-1: Preliminary Data Results

1. INTRODUCTION

The U.S. Air Force satellite P78-1 was launched at 0824 UT, 25 February 1979, into a circular, polar sun-synchronous orbit (noon-midnight meridian plane) at an altitude of 600 ± 30 km, inclination 97.73°. At launch, its period of revolution was 96.54 minutes. The satellite, shown in Figure 1, consists of a wheel section and a sail section.

The satellite carried several experiments, namely: solar x-ray and spectroheliograph; white light coronograph; XUV heliograph; near infrared spectrometer; x-ray monitor (auroral zone); x-ray and γ-ray spectrometers; electron, proton, and penetrating radiation spectrometers; a multiple particle analyzer and a set of two electron electrostatic analyzers. The electrostatic analyzers are being reported in this paper. They are on the rim of the wheel section, looking radially outward along the wheel's x and -y axes (within 3°). The spin axis of the wheel is perpendicular to the plane of the wheel section and directed along the plane of the sail. The spin rate of the wheel section is 11 ± 1 rpm, thus, the analyzers go through a full cycle of pitch angles approximately every 5.455 seconds.

This experiment can contribute greatly to an atlas of auroral zone and polar region precipitation in the noon-midnight meridian plane. Since the sensors are duplicates of the SSJ/3 sensor, a close comparison can be made when 78-1 and

(Received for publication 1 May 1981)

PRECEDING PAGE BLANK-NOT FILMED

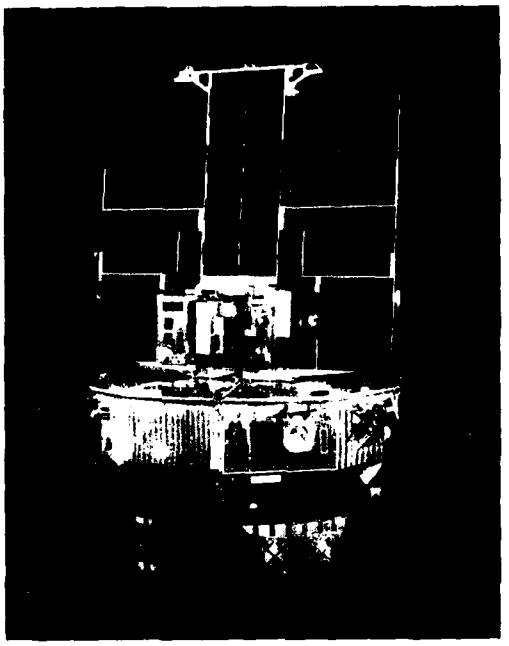

Figure 1. P78-1 Satellite

DMSP satellites are in close proximity in time and space. Since DMSP does not spin, the SSJ/3 sensor does not have variable pitch angle data, but does have excellent time resolution. Therefore, comparisons of the data from the two satellites can be made. In addition, DMSP auroral photographs can be compared with the 78-1 electron precipitation data in complete pitch angle distribution. The 78-1 data can also be compared with SCATHA particle data when the two satellites are in conjuction. The 78-1 ESA data can be compared with auroral x-ray and particle data observed on the 78-1 satellite.

2. DESCRIPTION OF ELECTROSTATIC ANALYZERS

The electrostatic analyzers flown on 78-1 are identical to the SSJ/3 analyzers previously flown on DMSP satellites and referred to as detectors 4 and 5 by Hardy et al.[1]

1. Hardy, D.A., Gussenhoven, M.S., and Huber, A. (1979) The Precipitating Electron Detectors (SSJ/3) for the Block 5D Flights 2-5 DMSP Satellites: Calibration and Data Presentation, AFGL-TR-79-0210, AD A083 136.

An average of the values given for these detectors in Hardy et al's Table 3 has been used to calculate the mid energy, energy width and the conversion factor from counts to differential number flux for each energy channel. Since

$$\frac{C \cdot \Delta T}{G(E_i)} \quad , \tag{1}$$

where $G(E_i)$ values are given in Table 3,[1] the conversion factor is

$$K \quad \frac{1}{\Delta T G(E_i)} \quad . \tag{2}$$

Table 1 lists these values for the 16 energy channels. It should be noted that the energy channels are listed here from low to high energy, whereas in Hardy et al[1] they are listed from high to low energy.

Table 1. The Conversion Factor, Mid-Energy, and Energy Width of Each Energy Channel

Channel	$K[(cm^2\ sec\ sr\ keV)^{-1}]$	E (keV)	ΔE (keV)
1	2.160×10^{7}	0.0468	0.0258
2	1.048×10^{7}	0.0726	0.0331
3	6.336×10^{6}	0.113	0.0502
4	4.399×10^{6}	0.173	0.0770
5	2.860×10^{6}	0.267	0.120
6	1.863×10^{6}	0.412	0.185
7	1.198×10^{6}	0.638	0.281
8	7.822×10^{5}	0.974	0.450
9	3.398×10^{5}	1.000	0.450
10	2.469×10^{5}	1.34	0.677
11	1.829×10^{5}	2.36	1.02
12	1.311×10^{5}	3.38	1.58
13	9.890×10^{4}	5.53	2.47
14	7.371×10^{4}	8.52	3.83
15	5.593×10^{4}	13.2	5.95
16	4.487×10^{4}	20.4	7.24

This electrostatic analyzer experiment consists of a set of four analyzers that perform a differential energy analysis of electrons simultaneously in two look directions. A 16-point spectrum is produced for each look direction every 256 msec by low and high energy analyzers that are of a conventional curved plate design with balanced positive and negative deflection voltages. The instrument is designed to collect electrons in the energy range of approximately 50 eV to 20 keV. One set of plates collects electrons in eight channels between 50 eV and 1 keV and the second set collects electrons in eight channels from 1 to 20 keV. A second set of analyzers is 90° from the first set. Both sets are mounted perpendicular to the spin axis of the wheel section and, therefore, rotate through the full cycle of pitch angles, one set leading by 90°, on each spin cycle. The voltage applied to determine the channels energy is swept simultaneously for the four analyzers. The total weight of the experiment is 4.34 lb, and it is contained in a box 6" × 6" × 4.187". The power dissipation is 0.25 W at 28 V dc. The dwell time on each channel is 27 msec, with 5 msec between steps to stabilize the voltage. Thus, in each wheel spin cycle, each detector gives nearly 22 sixteen-point spectra. A full description and calibration technique of the instrument are given by Hardy et al[1] and Huber et al.[2]

Using the values in Table 1, $j(E_i)$, the differential number flux, is expressed in electrons $(cm^2\ sec\ sr\ keV)^{-1}$. The integral (total number) flux is given by:

$$J_{TOT} = \sum_i j(E_i)\,\Delta E_i \qquad e\ (cm^2\ sec\ sr)^{-1} \quad . \tag{3}$$

The integrated energy flux is:

$$J_{ETOT} = \sum_i j(E_i)\,\Delta E_i \cdot E_i \qquad keV\ (cm^2\ sec\ sr)^{-1} \tag{4}$$

and the average energy is:

$$E_{AV} = \frac{J_{ETOT}}{J_{TOT}} \qquad keV \quad . \tag{5}$$

---

2. Huber, A., Pantazis, J., Besse, A. L., and Rothwell, P. L. (1977) Calibration of the SSJ/3 Sensor on the DMSP Satellites, AFGL-TR-77-0202, AD A045 997.

[illegible]

[illegible] OF MEASUREMENTS FROM THREE PASSES

[illegible]

[illegible] Rev 270 Kp [illegible] 13 Mar 1970

[illegible]

[illegible] The satellite passes across the dayside oval just past noon CGM local time, [illegible] [illegible] CGM [illegible] [illegible] needs into the late evening oval very near midnight, CGM local time. The oval appears to be very narrow throughout and poleward, as expected for Kp [illegible].

As the vehicle approaches the dayside oval boundary, the total particle flux, J_{TOT} is $< 10^7$ e (cm^2 sec sr)$^{-1}$, as seen in Figure 3. At 46,478.2 sec UT, J_{TOT} becomes $>10^7$ (CGM latitude 7[illegible].8°) and remains $>10^7$ until 4[illegible],[illegible]87.[illegible] sec UT (CGM latitude 83.[illegible]°) when it falls abruptly to $<10^7$ e (cm^2 sec sr)$^{-1}$. At this time, it enters the polar cap region. At 46,964.7 sec UT (CGM latitude 71.[illegible]°), J_{TOT} rises abruptly to $>10^7$ and remains so until 47,02[illegible].7 sec UT (CGM latitude 67.9°). In this latter period, the satellite passes through the nighttime oval. In Table 2, these values are shown with Whalen's values for Kp 0_+. The latitude values given above are at ground level directly below the satellite. Table 2 lists these and the values that the field lines intersecting the satellite position reach at

---

3. Whalen, J.A. (1970) Auroral Oval Plotter and Nomograph for Determining Corrected Geomagnetic Local Time, Latitude and Longitude for High Latitudes in the Northern Hemisphere, AFCRL-70-0422, AD 713 170.

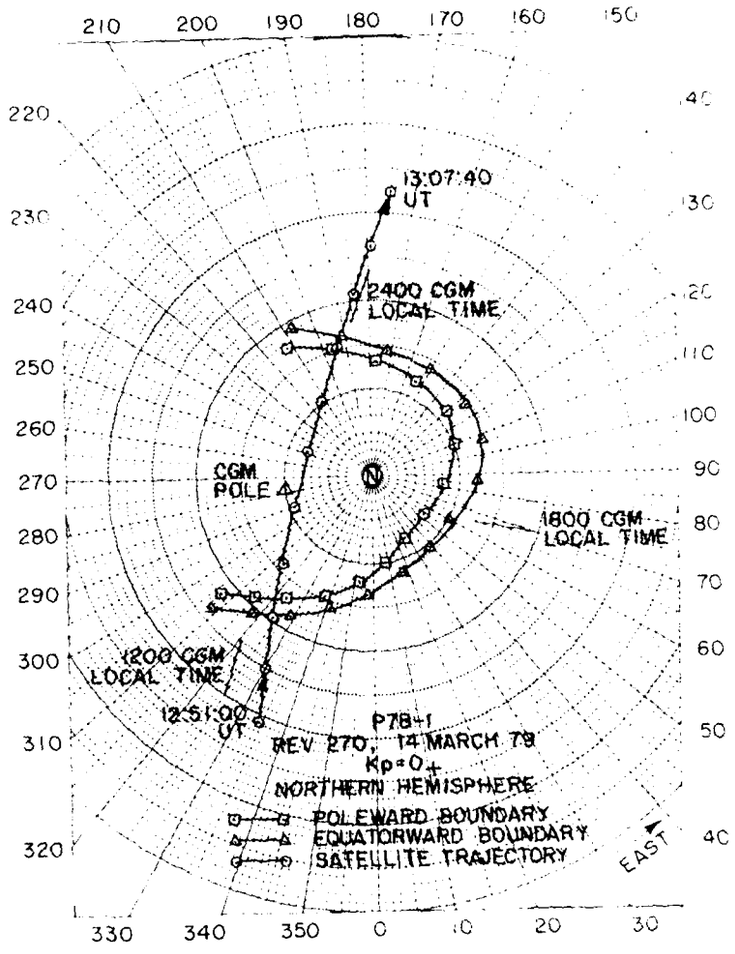

Figure 2. Trajectory in Northern Auroral Zone for Rev 270, 14 March 1979

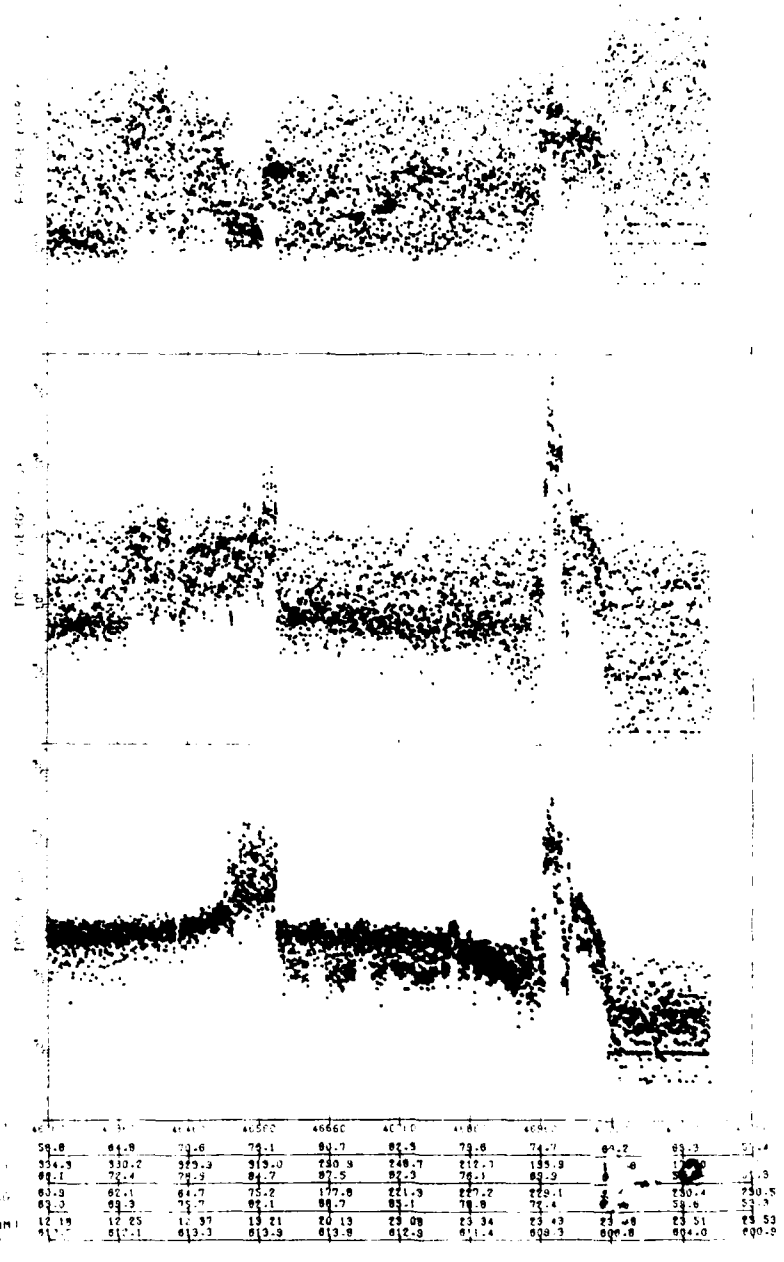

Figure 3. Electron Data From Rev 270, 14 March 1979, During a Magnetic Quiet Time, Kp = 0_+. Data was taken in the northern hemisphere

Table 2. Rev 270 (Kp 0_+). CGM Latitudes for Dayside and Nightside Auroral Oval Boundaries

	Ground Level Below Satellite	Field Lines at Satellite Intersect Ground	Whalen's Ground Level Values
Equatorward Boundary (Day)	76.8°	77.4°	75.8°
Poleward Boundary (Day)	83.6°	83.9°	77.5°
Poleward Boundary (Night)	71.9°	72.6°	71.8°
Equatorward Boundary (Night)	67.9°	69.0°	70.1°

ground level. Also shown are Whalen's values at ground level for these times and positions.

Figure 4a shows an electron spectrum from each detector. Both spectra consist of electrons that are nearly field-aligned, as seen from their pitch angle ranges, and are 1.280 sec apart in universal time. There is good agreement and both show a flux peak at ~2.4 keV. The total energy flux at this time is $J_{ETOT} \approx 1$ erg $(cm^2 \text{ sec sr})^{-1}$. This would indicate that the auroral form is a moderate discrete arc.[4]

Figure 4b shows both detectors sweeping simultaneously for two successive sweeps. In the first sweep detector 1 is closer to field-aligned pitch angles, and in the second sweep detector 2 is closer to field-aligned values. In the first sweep, detector 1 runs slightly lower than detector 2 at most energies. In the second sweep, detector 2 runs somewhat higher in the lower energies, as one would expect since it is nearly field-aligned. The values in the higher energy analyzers are quite close. These spectra show a peak in the flux, and it is more pronounced in the first sweep of each detector. These observations were made close to the poleward boundary of the nightside oval.

Figure 5a shows a spectrum observed by detector 1 near the equatorward boundary. The fluxes are weak, with a maximum flux occurring at ~1.0 keV and $J_{ETOT} \approx 0.1$ erg $(cm^2 \text{ sec sr})^{-1}$. This could be a faint discrete arc, since a peak occurs near 1 keV and the energy flux is a fraction of an erg $(cm^2 \text{ sec sr})^{-1}$.

4. Meng, C-I. (1980) Auroral arcs observed by DMSP satellites, geophysical monograph in Proceedings of the Chapman Conference on the Foundation of Auroral Arcs, submitted November 1980.

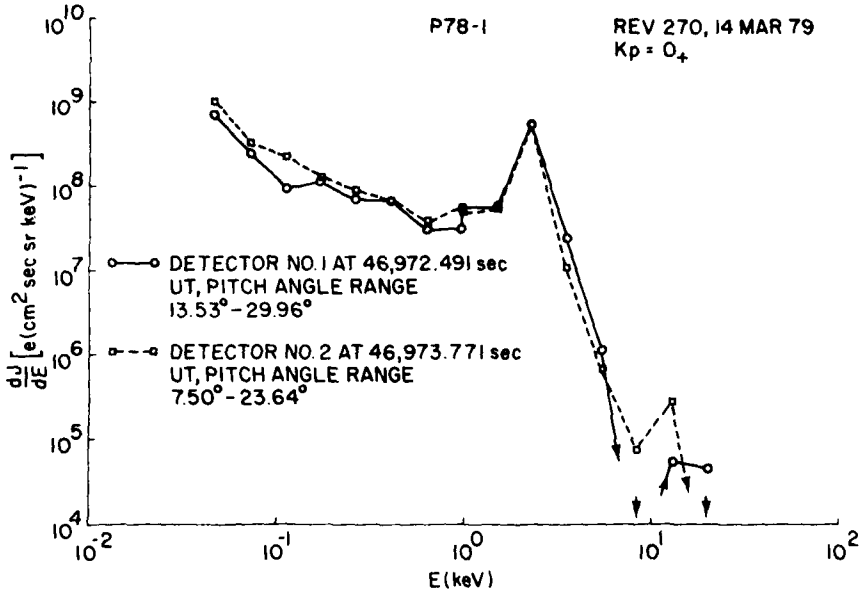

Figure 4a. Differential Electron Spectra From Both Detectors at Corrected Geomagnetic Latitude 70.7°, Northern Nightside Auroral Oval, Rev 270, 14 March 1979. Spectra are due to electrons that are nearly field-aligned

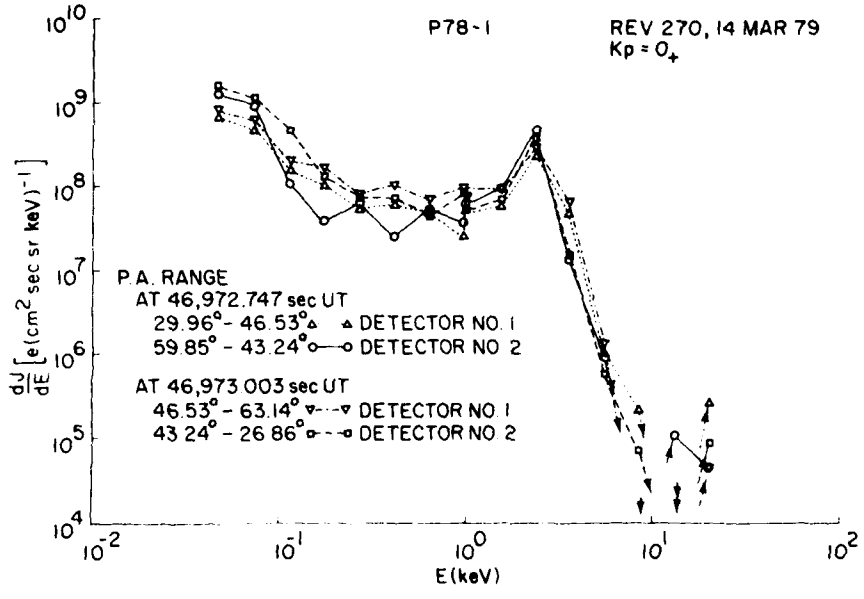

Figure 4b. Same as 4a Except Electrons are not Field-Aligned but Were Collected Simultaneously With Approximately Equal Pitch Angles for Both Detectors

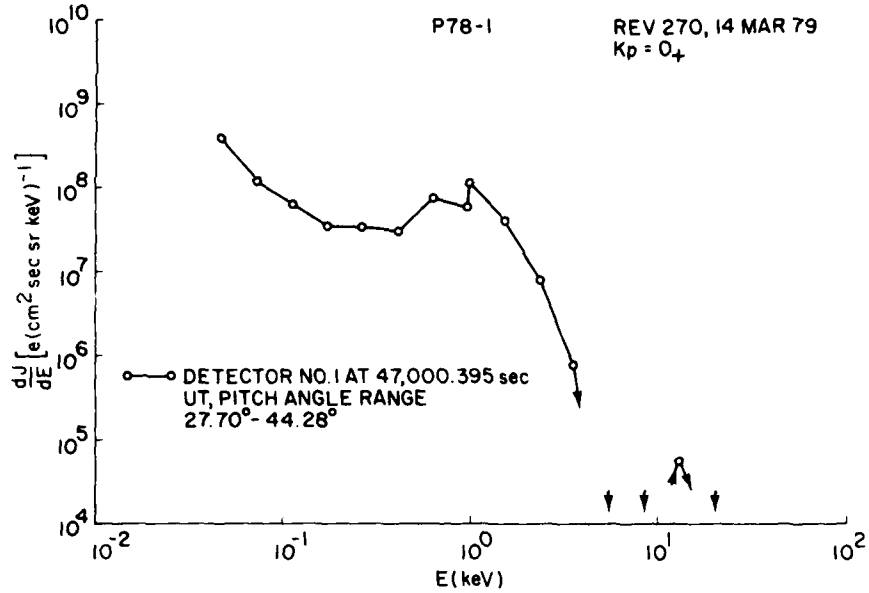

Figure 5a. Differential Electron Spectrum Taken at Corrected Geomagnetic Latitude 69.0°, Rev 270

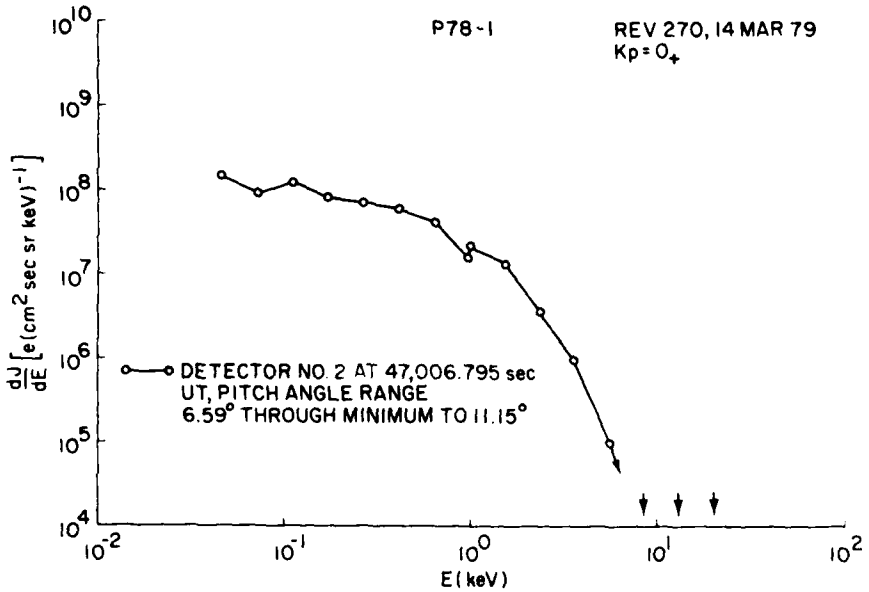

Figure 5b. Differential Electron Spectrum From Detector 2 Taken at Corrected Geomagnetic Latitude 68.5°, Rev 270. Electrons are field-aligned

Figure 5b was taken 6.400 sec later by detector 2. It is a weak flux with no peak and, since $J_{ETOT} \approx 0.03$ erg $(cm^2 \text{ sec sr})^{-1}$, it corresponds to a weak diffuse auroral form. This occurs just inside the equatorward boundary of the nightside oval. This orbit shows the discrete and diffuse forms to be in those regions of the nightside oval where one expects them to be.

3.2 Moderate Activity (Rev 220, Kp = 3_+), 11 March 1979

Figure 6 shows the trajectory for Rev 220, 11 March 1979. The satellite enters the dayside oval near CGM local time 0900 at 10,960.8 sec UT and at CGM latitude 72.3°. As seen in Table 3, this agrees with Whalen for Kp = 3_+. According to Whalen's values and this trajectory, the satellite should pass by the poleward boundary at 11,034.8 sec UT (CGM latitude 74.5°), but Figure 7 shows such variability in J_{TOT} that the poleward boundary of the day and night sides cannot be determined from the J_{TOT} vs time plot. As shown in Figure 6, the satellite moves only slightly poleward of Whalen's poleward boundary. Possibly the satellite is moving in and out of the boundary, particularly if the boundary varies in time or location. This could account for the changes in flux in Figure 7 which occur from the dayside poleward edge to the nightside poleward edge. Thus, the nightside poleward boundary is also obscured. According to Whalen's values and the trajectory, the satellite should enter the nightside oval at 11,405.0 sec UT (CGM latitude 71.8°). The equatorward boundary of the nightside is shown in Figure 7 by an abrupt drop in J_{TOT} at 11,566.3 sec UT (CGM latitude 65.8°). One can see the broadening of the oval and the equatorward shift for Kp = 3_+ (Figure 6) relative to Kp = 0_+ (Figure 2). Table 3 shows the values of the boundaries.

Table 3. Rev 220 (Kp = 3_+). CGM Latitudes For Equatorward Auroral Oval Boundaries

	Ground Level Below Satellite	Field Lines at Satellite Intersect Ground	Whalen's Ground Level Values
Equatorward Boundary (Day)	72.3°	73.1°	72.3°
Equatorward Boundary (Night)	65.8°	66.9°	64.3°

Figure 8a shows an electron spectrum from each detector. Detector 1 passes through field-aligned pitch-angle values 1.280 sec before detector 2. The

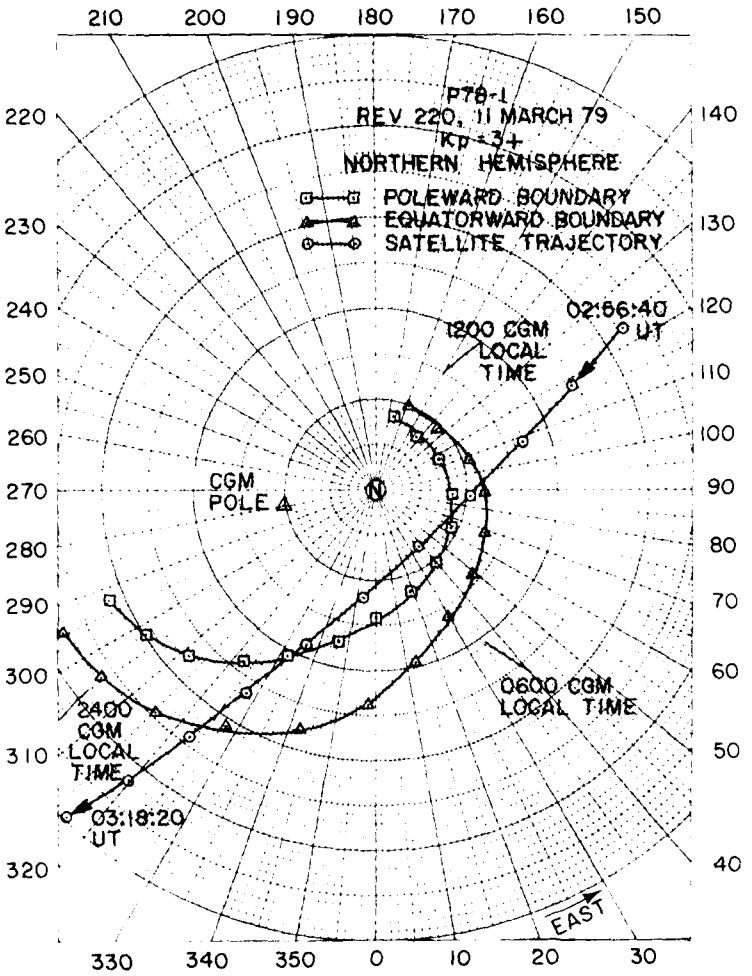

Figure 6. Trajectory in Northern Auroral Zone For Rev 220, 11 March 1979

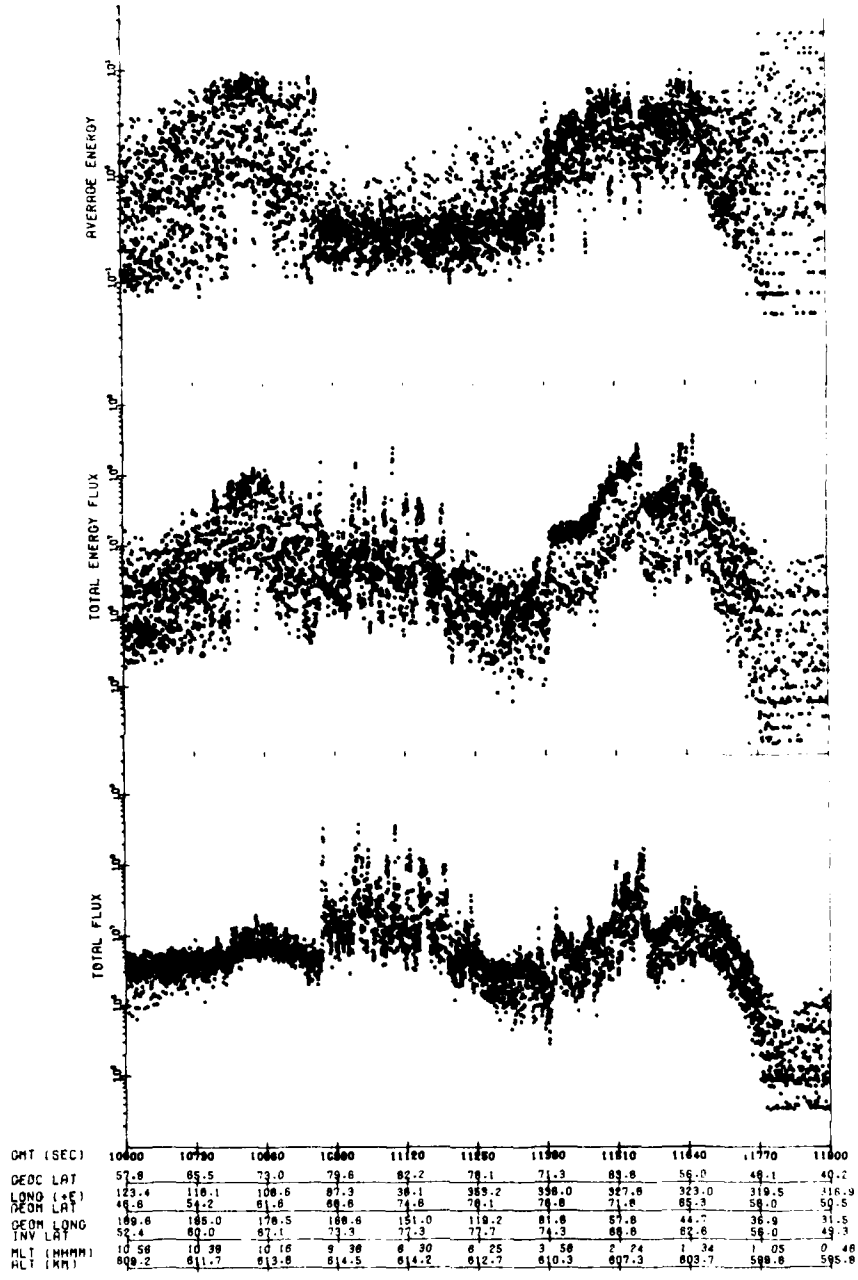

Figure 7. Electron Data From Rev 220, 11 March 1979, During a Magnetically Moderate Time, Kp = 3_+. Data was taken in the Northern Hemisphere

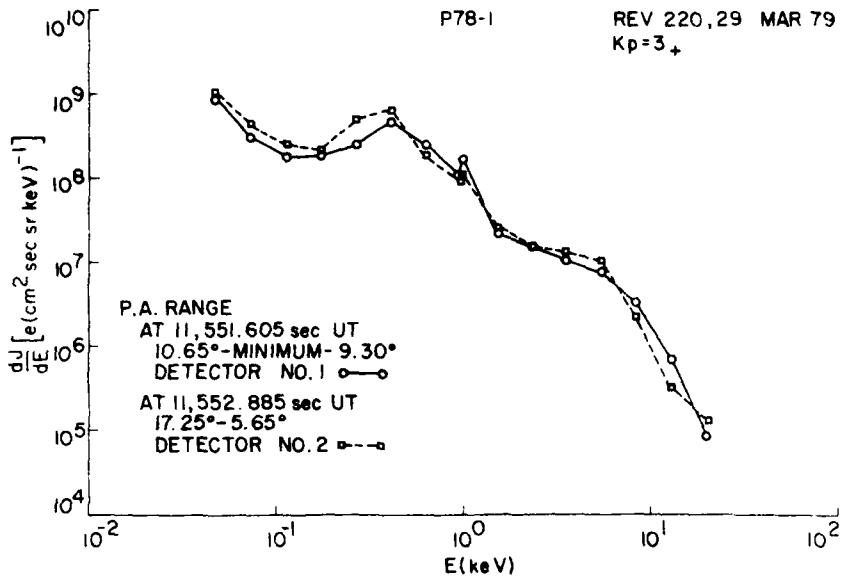

Figure 8a. Differential Electron Spectra From Both Detectors Taken at Corrected Geomagnetic Latitude 66.4°, Northern Nightside Auroral Oval, Rev 220. Electrons are field-aligned

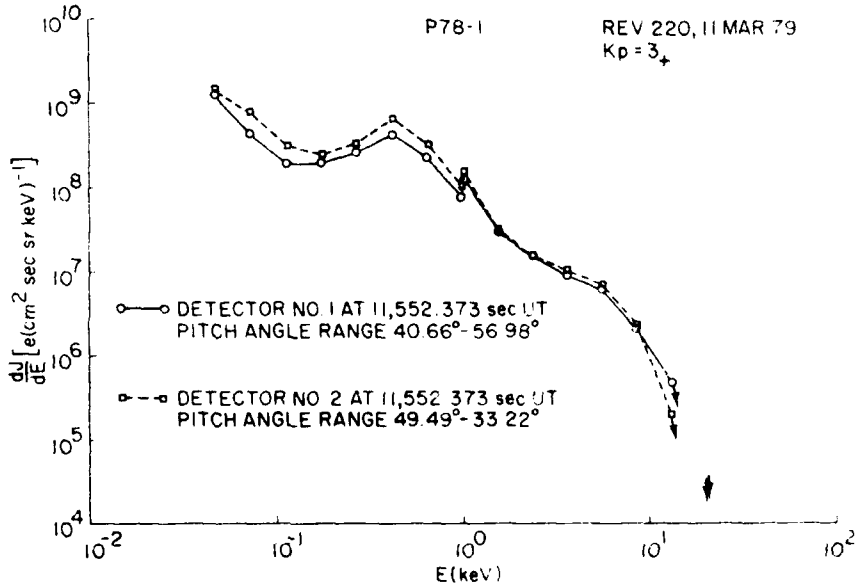

Figure 8b. Same as 8a Except Electrons Are Not Field-aligned but Were Collected Simultaneously With Approximately Equal Pitch Angles for Both Detectors

two are seen to be quite similar. In Figure 8b, the two detectors are measuring simultaneously at approximately the same pitch angles, and the agreement is very good. There are slight peaks in flux at ≈ 0.41 keV and the energy flux is $J_{ETOT} \approx 0.3$ erg $(cm^2 \text{ sec sr})^{-1}$. This would appear to be a diffuse auroral form. These spectra are near the equatorward boundary. Since no spectra with peaked fluxes were observed in this nightside oval passage, it is assumed that the satellite did not pass over any discrete forms.

3.3 Intense Activity (Rev 499, Kp = 7_), 29 March 1979

Figure 9 shows the trajectory in the southern hemisphere for Rev 499 on 29 March 1979. This took place during a magnetic storm at a time when Kp = 7_. The oval boundaries shown are from Whalen and are seen to broaden and move equatorward of the previous two cases. However, the satellite electron total fluxes show that the increase in total flux starts more equatorward and drops abruptly more equatorward than Whalen shows. Thus, from Hardy's criteria, in this case the oval is broader and more equatorward during this storm time than Whalen has shown for the oval for Kp = 7_. From Figure 10, the fluxes show that the satellite enters the nightside oval at 65, 118.5 sec UT (CGM local time ≈ 2300) and at CGM latitude 53.9° South. At 65, 390.0 sec UT (CGM local time ≈ 2200), J_{TOT} drops abruptly below 10^7 e $(cm^2 \text{ sec sr})^{-1}$ indicating the poleward boundary at CGM latitude 67.0°. At 65, 931.9 sec UT (CGM local time ≈ 1500), J_{TOT} rises above 10^7 e $(cm^2 \text{ sec sr})^{-1}$ indicating the poleward boundary of the dayside oval at CGM latitude 66.7°. At 66, 019.3 sec UT (CGM local time ≈ 1430), J_{TOT} abruptly falls again below 10^7, showing the equatorward boundary at CGM latitude 62.7°. Table 4 shows the oval boundary values.

Figure 11 shows differential electron spectra from each detector taken simultaneously at approximately the same pitch-angle range. Detector 2 is somewhat higher in the low energy range, but there is good agreement in form. The peak in Channel 5 (0.173 keV) detector 2 is due to that channel having higher counts than usual, even when the sensor is looking toward earth. Both show a weak diffuse aurora at CGM latitude 56.0° near the equatorward edge of the nightside oval.

Figure 12 shows a spectrum from detector 1 taken more than a minute after the spectra in Figure 11. This spectrum shows a broad peak in flux at 3.5 keV when $J_{ETOT} \approx 2.80$ erg $(cm^2 \text{ sec sr})^{-1}$. This occurs at CGM latitude 59.3° and would be associated with a moderate discrete arc.

Figure 13 shows differential spectra from detector 2 taken during three successive rotations for field-aligned electrons. One spectrum is from detector 1 and is taken in the same time period. The first spectrum (solid line) shows a gradual increase and peaks at 8.5 keV. The dashed line (second spectrum) shows

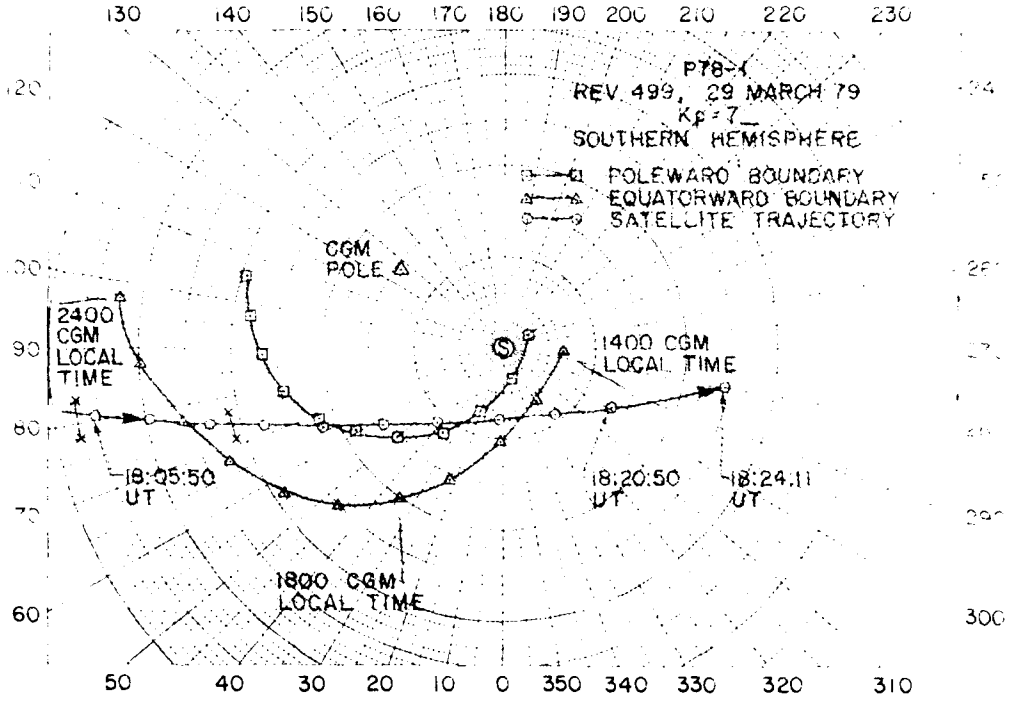

Figure 5. Trajectory in Southern Auroral Zone [illegible]

Table 4. Rev 499 (Kp = 7-). CGM Latitudes for Dayside and Nightside Auroral Oval Boundaries

	Ground Level Below Satellite	Field Lines at Satellite Intersect Ground	Whalen's Ground Level Values
Equatorward Boundary (Night)	53.9°	55.7°	61.8°
Poleward Boundary (Night)	67.0°	68.1°	73.5°
Poleward Boundary (Day)	66.7°	67.8°	72.2°
Equatorward Boundary (Day)	62.7°	64.0°	68.8°

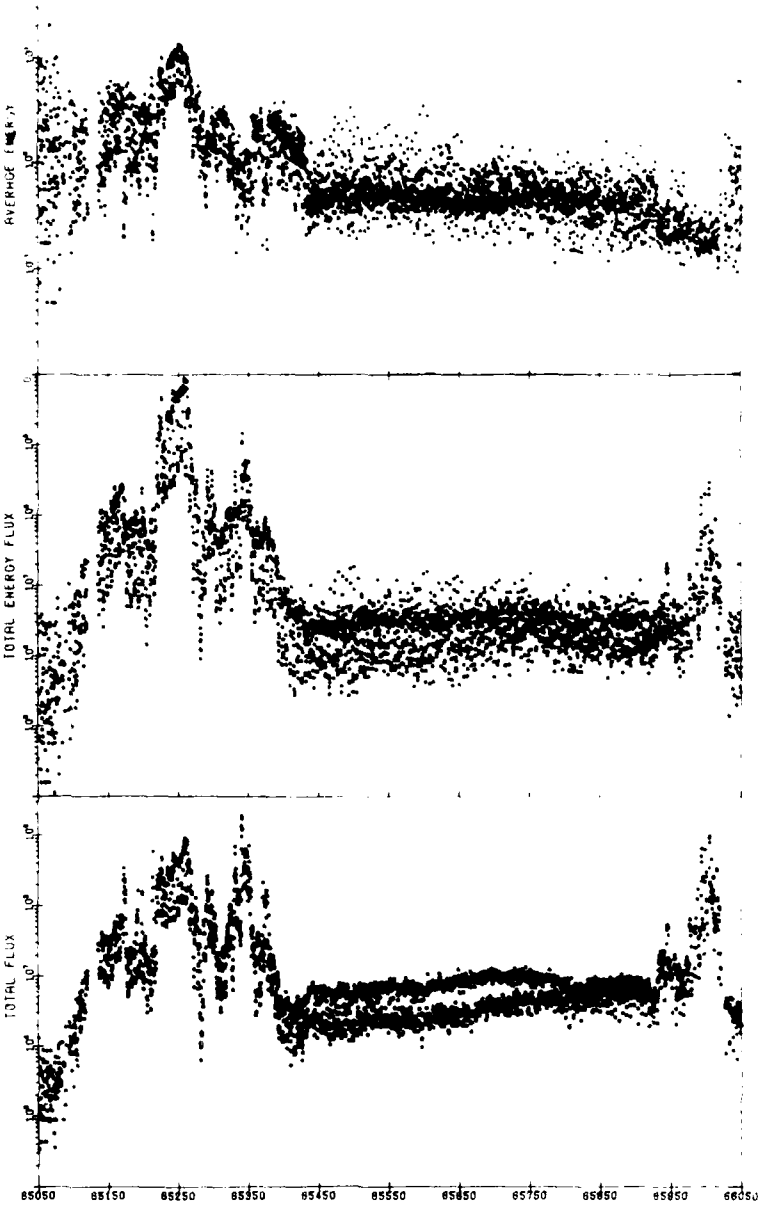

GMT (SEC)	65050	65150	65250	65350	65450	65550	65650	65750	65850	65950	66050
GEOC LAT	-38.4	-44.8	-50.7	-56.7	-62.8	-68.8	-74.9	-79.9	-82.2	-80.9	-76.5
LONG (+E)	82.8	80.7	78.5	75.7	71.9	66.6	57.8	40.7	4.6	322.5	298.8
GEOM LAT	-48.4	-54.9	-60.0	-65.5	-70.5	-74.8	-77.4	-77.9	-74.5	-70.2	-65.2
GEOM LONG	145.9	142.1	137.2	130.5	120.5	104.9	80.9	52.3	28.1	14.0	4.3
INV LAT	51.9	57.5	62.8	67.1	70.7	73.2	74.0	73.0	70.4	66.7	62.4
MLT (HHMM)	23 14	23 01	22 43	22 18	21 40	20 38	19 06	17 12	15 41	14 42	14 05
ALT (KM)	578.1	579.4	582.7	585.9	588.2	592.8	598.0	598.4	602.6	605.4	607.6

Figure 10. Electron Data From Rev 499, 29 March 1979, During a *Magnetic Storm Time, Kp = 7+. Data were taken in the southern* hemisphere

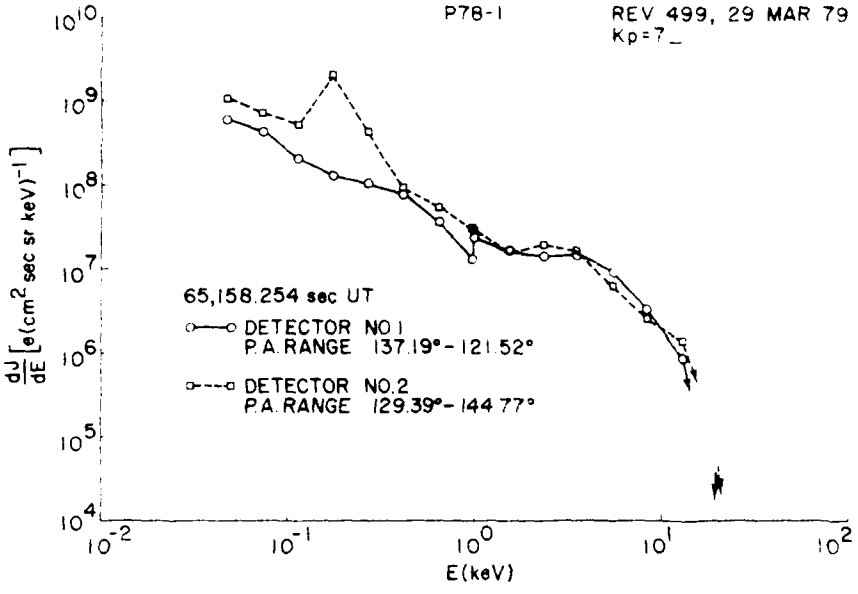

Figure 11. Differential Electron Spectra From Both Detectors at Corrected Geomagnetic Latitude 56.0° South, Near Equatorward Edge of Nightside Oval, Rev 499. Spectra were taken simultaneously at approximately the same pitch angles

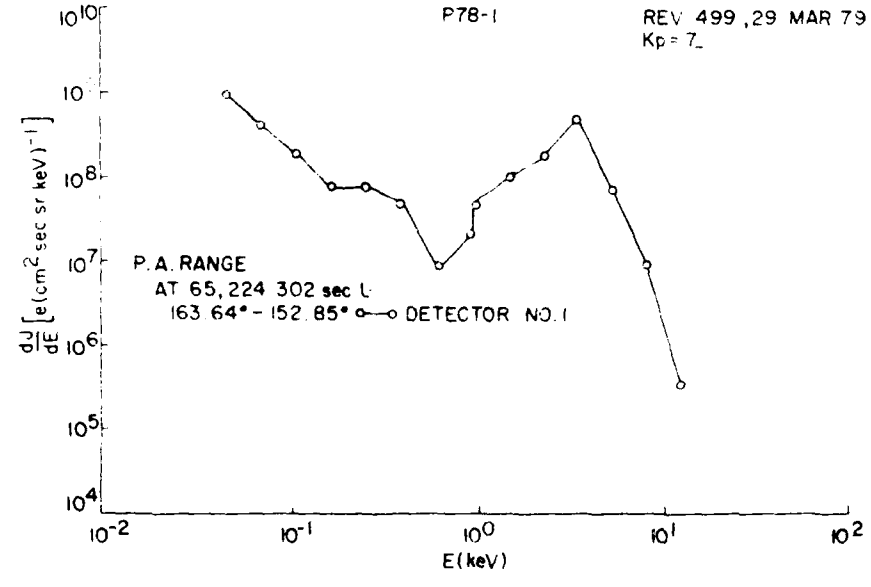

Figure 12. Differential Electron Spectrum From Detector 1 Taken at Corrected Geomagnetic Latitude 59.3°, Rev 499. Electrons are nearly field-aligned

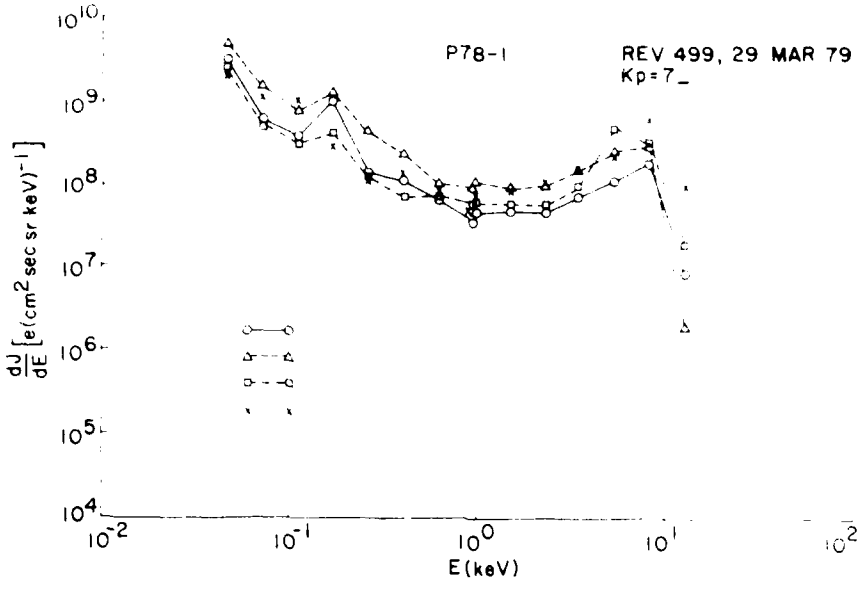

Figure 13. Differential Electron Spectra From Detector 2 Taken During Three Successive Rotations of the Satellite. The fourth spectrum is from detector 1 during an intermediate time period. All spectra are due to field-aligned electrons, Rev 499. Corrected Geomagnetic Latitude 60.9° to 61.3°

the same gradual increase, but it flattens out between 5.5 and 8.5 keV. The third spectrum (dotted line) shows a much narrower peak at 5.5 keV. During the first and second spectrum, $J_{ETOT} \approx 8.5$ erg (cm^2 sec sr)$^{-1}$, and during the third, $J_{ETOT} \approx 4.4$ erg (cm^2 sec sr)$^{-1}$. Thus, as the peak shifted to lower energies, J_{ETOT} decreased. This would be associated with an intense discrete arc that was lessening to a moderate discrete arc. The spectrum shown by the marks of an x is from detector 1. It was taken between the first and second spectrum of detector 2 and shows a peak at 8.5 keV and $J_{ETOT} \approx 13.8$ erg (cm^2 sec sr)$^{-1}$ which, also, indicates an intense discrete arc. All four spectra were of field-aligned electrons and were taken from CGM latitudes 60.9° to 61.3°.

Figure 14 is a plot of the values of the electron energy where the maximum flux occurred (precipitating electrons only) versus universal time in seconds for Rev 499. Thus, these electrons are from the upper hemisphere of pitch angles. There is a narrow peak to 7.4 keV at ≈ 65,225.5 sec UT. As seen in the plot, the energy peak value increases from 65,235.6 sec UT to 65,241.7 sec UT to a value of ≈ 8.3 keV and then levels off until 65,254.0 sec UT when it falls quickly. It was during the period of maximum that the curves in Figure 13 were obtained.

Figure 15 is a differential spectrum from detector 1 and shows a somewhat broad peak at ≈ 1.3 keV when $J_{ETOT} \approx 0.7$ erg (cm^2 sec sr)$^{-1}$. This would

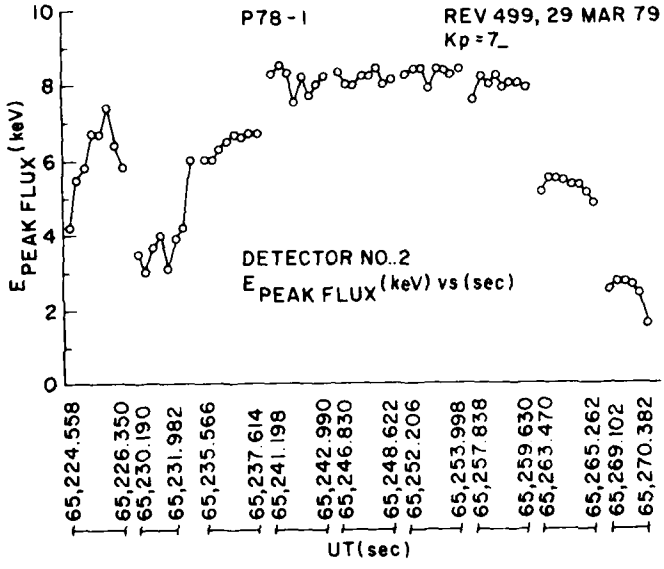

Figure 14. Plot of Electron Energy Values Where Maximum Flux Occurred Versus Universal Time in Seconds, Rev 499, Southern Nightside Auroral Oval, Active Region

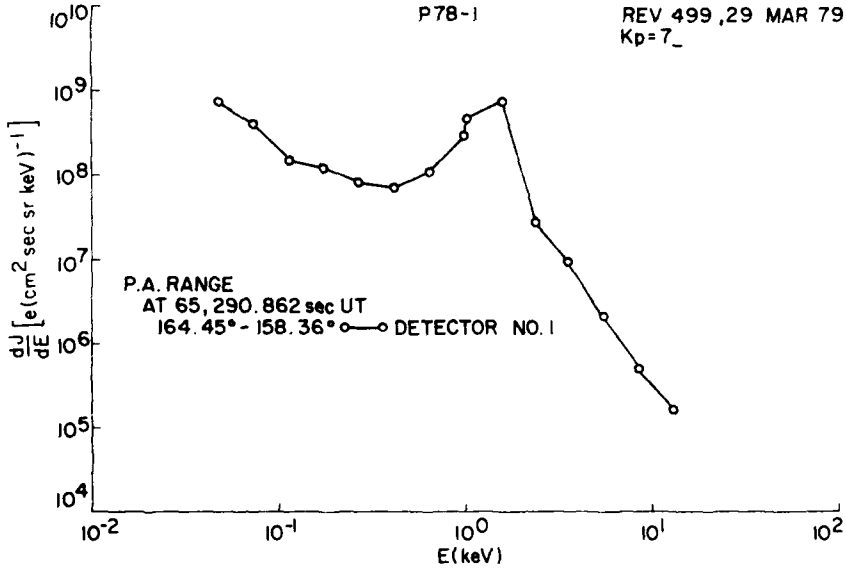

Figure 15. Differential Electron Spectrum From Detector 1 Taken at Corrected Geomagnetic Latitude 62.6°, Rev 499. Electrons are nearly field-aligned

indicate a weak discrete arc. The electrons were nearly field-aligned and the spectrum occurred at CGM latitude 62.6°.

Figure 16 shows differential spectra from each detector. They were taken simultaneously and at approximately the same pitch-angle range. There is a small but real increase in flux at 0.64 keV ($J_{ETOT} \approx 2$ erg $(cm^2\ sec\ sr)^{-1}$). This is probably a weak discrete arc at 64.8° CGM latitude. Again in the lower energy range, detector 2 is running higher, but the shape of the spectra is very much alike and the agreement is excellent in the high energy range.

Figure 17 shows a spectrum from detector 1 of nearly field-aligned electrons. This spectrum has no peak in flux and $J_{ETOT} \approx 0.2$ erg $(cm^2\ sec\ sr)^{-1}$, which indicates a diffuse auroral form. This occurred near the poleward edge of the nightside oval at ≈ 65.6° CGM latitude.

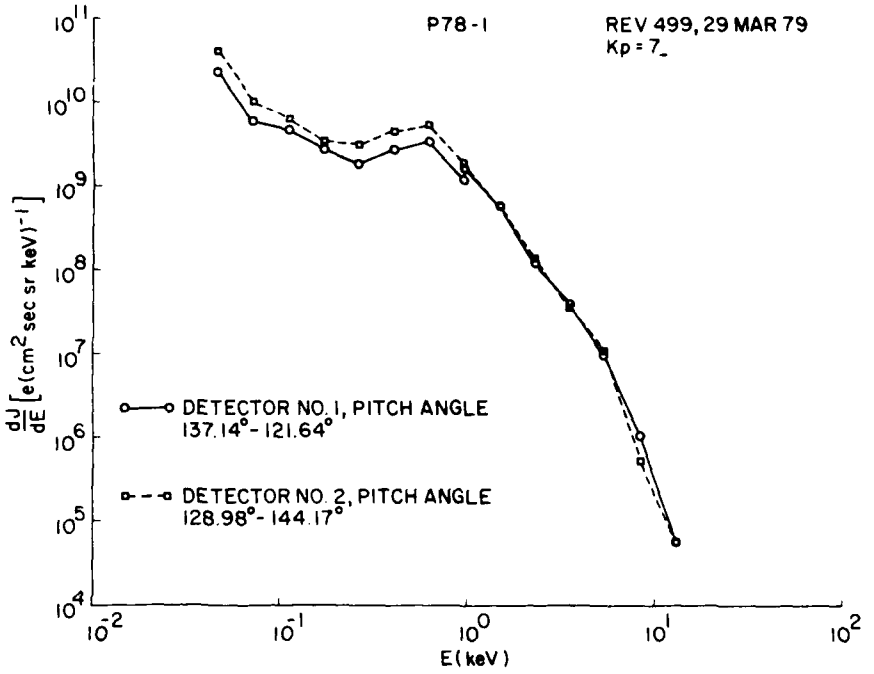

Figure 16. Differential Electron Spectra From Both Detectors Taken at Corrected Geomagnetic Latitude 64.8°, Southern Nightside Auroral Oval, Rev 499. Electrons are not field-aligned but were collected simultaneously with approximately equal pitch angles for both detectors

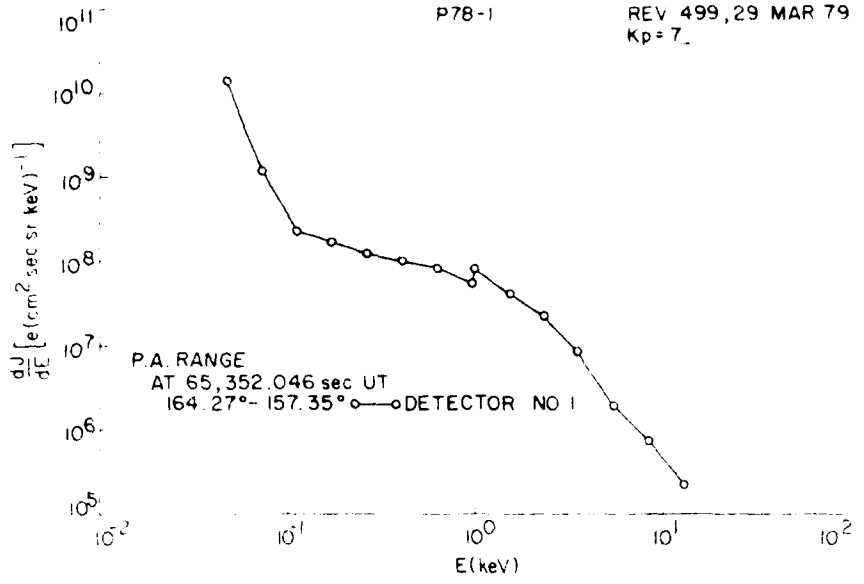

Figure 17. Differential Electron Spectrum From Detector 1 Taken at Corrected Geomagnetic Latitude [illegible], Rev 499. Electrons are nearly field-aligned.

4. CONCLUDING REMARKS

Precipitating electron data have been analyzed for three 78-1 satellite passes each for a different type of magnetic activity. In the first, Rev 270, Kp = 0_+ (quiet), the observed auroral boundaries agree quite well with those of Whalen, except the dayside poleward boundary. However, the poleward boundary from this data is shown quite clearly by an abrupt drop in J_{TOT}, the total electron flux. The drop also agrees with Hardy's criterion of being less than 10^7 e (cm^2 sec sr)$^{-1}$. The two detectors give similar shaped spectra with flux peaks occurring at the same energy, and with approximately the same total energy flux, J_{TOT}.

In Rev 220, Kp = 3_+ (moderate), the satellite trajectory passed well morningside of the CGM North Pole and very close to the oval poleward boundary. Since the J_{TOT} vs t curve, Figure 7, shows many fluctuations, the poleward boundaries of the day and night sides are difficult to determine. However, the equatorward boundaries are obvious from the sudden change in J_{TOT} and agree very well with Hardy's criterion and Whalen's values, as seen in Table 3.

Even though Kp = 3_+, no discrete aurora was observed on this northern auroral nightside oval pass. This is not uncommon for Kp = 3_+.

In Rev 499, Kp 7_- (disturbed) and, using the J_{TOT} plot and Hardy's criterion, the dayside boundaries are more than 4° equatorward and the nightside boundaries more than 5° equatorward of Whalen's values. It would appear from the abruptness of the change in J_{TOT} that Hardy's criterion of 10^7 e (cm^2 sec sr)$^{-1}$ is quite accurate. The equatorward shift of the oval is as expected for the high value of Kp 7_-.

Figures 11 to 13 and 15 to 17 show samples of spectra of auroral forms in different parts of the nightside oval. It is seen that discrete auroral forms of varying intensity occurred throughout most of this nightside oval, except near the equatorward boundary where the diffuse form is found as expected. Some diffuse aurora was found near the poleward edge of the nightside (Figure 17). The activity in this pass would seem to be associated with either a substorm breakup or post-breakup period because of its wide extent in the south-north direction, the high energy peaks, and the high Kp value.

When comparing the fluxes measured by the two detectors, it is observed that detector 2 reads about 40 percent higher than detector 1 in the lower energy range, channels 1 through 8 (50 eV to 1 keV). This happened throughout most of the three passes. In the higher energy range, there was very close agreement between the two detectors.

In Rev 499, channel 4 read high throughout the southern auroral oval pass that we discussed above. That was true in both detectors, but because detector 2 read higher than detector 1, the J_{TOT} values for detector 2 were $>10^7$ e (cm^2 sec sr)$^{-1}$ throughout this pass. Therefore, we used detector 1 data in Figure 10. It must be stressed that channel 4 does not generally act this way.

Originally, it appeared that Channel 9 was not functioning properly. It was suggested by Dr. Hardy that the data was taken off of telemetry in a manner such that channels 8 and 16 were interpreted as being channels 1 and 9, respectively. All other channels were then corrected accordingly and, therefore, all channels function properly.

Since the launch of satellite P78-1, this experiment has produced some very good data. Due to the geometric factors for the low energies, these detectors can detect very low fluxes throughout the entire spectrum and very high fluxes in the lower energies. Thus, complete spectra can be produced in the polar cap and the cusp. Flux spectra are produced throughout the entire spin cycle. This indicates that they can be used to estimate the field-aligned current densities.